Temperature-robust multivariate calibration

Wülfert, F.

Publication date
2004

2. INFLUENCE OF TEMPERATURE ON VIBRATIONAL SPECTRA AND CONSEQUENCES FOR THE PREDICTIVE ABILITY OF MULTIVARIATE MODELS.

Abstract

Temperature, pressure, viscosity and other process variables fluctuate during an industrial process. When measuring vibrational spectra on- or in-line for process analytical and control purposes, the fluctuations influence the shape of the spectra in a non-linear manner. The influence of these temperature induced spectral variations on the predictive ability of multivariate calibration models is assessed. Short wave NIR spectra of ethanol/water/2-propanol mixtures are taken at different temperatures and different local and global partial least squares calibration strategies are applied. The resulting prediction errors and sensitivity vectors of a test set are compared. For data with no temperature variation, the local models perform best with high sensitivity but the knowledge of the temperature for prediction measurements cannot aid in the improvement of local model predictions when temperature variation is introduced. The prediction errors of global models are considerably lower when temperature variation is present in the dataset but at the expense of sensitivity. In order to be able to build temperature-stable calibration models with high sensitivity, a way of explicitly modeling the temperature should be found.

Based on: Wülfert, F.; Kok, W.Th.; Smilde, A.K.; *Anal. Chem.* **1998**, *70*, 1761-1767.

Introduction

General

Mid infrared, Near-Infrared (NIR) and short-wave NIR spectroscopic techniques in combination with multivariate calibration are finding an increasing range of applications in process analysis [1, 2, 3, 4, 5, 6, 7]. The spectroscopic analysis can be done in- or on-line and, in contradiction to slower classical off-line techniques, the results can be used for process control purposes.

The high sensitivity and consequently short pathlengths (in the range of a few μm) of mid-IR instrumentation is often not compatible with industrial environments. With the orders of magnitude lower absorbance of the overtones in NIR and short-wave-NIR , much more robust flow cells can be used which are not susceptible to blockage.

By moving the measurement from the well controlled laboratory to the process environment, external process variables such as temperature, pressure, flow turbulence will also affect the measurements. The difficulty to keep these variables constant or even the inevitability to change their value during the process (e.g. temperature programming in batch processes) makes it necessary to study the influence on the spectra and therefore also on the calibration models.

Temperature effects on vibrational spectra

Vibrational spectra from liquid and solid samples do not only show isolated molecular features, such as structure and functional groups, but also inter- or intramolecular features, such as hydrogen bonding. These weaker forces influence the vibrational modes[8, 9, 10, 11, 12, 13, 14, 15, 16, 17] of molecular bonds but are themselves affected by conditions such as temperature and pressure. Therefore the variations in, e.g., temperature translate via the changes in intermolecular forces to modifications of the vibrational spectra.

The influence of the temperature on the O-H stretch band and its overtones has been described in various articles[18, 19, 20, 21, 22]. The hydroxyl group gives rise to two bands for its stretching mode: a sharper band for the "free" O-H groups and a broader one for the stretch mode of hydrogen-bonded O-H groups. The broad band, which can be seen as an overlay of many bands that belong to different cluster sizes formed by hydrogen bonding, is shifted towards lower energies (higher wavelength) relative to the free O-H stretch. Rising the temperature decreases the average cluster size and increases the relative absorbance of free groups[23].

This can be seen most clearly in water spectra where the hydroxyl band shifts to the lower wavelengths and becomes sharper when the temperature is increased. The increase of free O-H groups can also be observed for alcohols, but a combination C-H stretch mode that absorbs in the same region makes the effect less apparent. Similar effects can be observed for spectra of polyamides and polyurethane, where the N-H groups can form hydrogen bonds[24, 25, 26]. The bands originating from N-H stretching modes are influenced by the temperature much in the same way as for hydroxyl groups.

Effects of shifts and peak distortion on multivariate regression

Due to a lack of selectivity NIR applications consist mostly of spectroscopic measurements in combination with multivariate data analysis. Partial Least Squares (PLS) and Principal Component Regression (PCR) are the most common methods. Both methods assume linear additivity. This means that absorption spectra are supposed to increase linearly with the concentration (linearity) and that a mixture of components gives a spectrum that is a linear combination of the pure spectra (additivity). Any deviation from this ideal behavior has to be approached by using more components in the PLS or PCR model.

Spectra that exhibit shifts or other changes in their shape do not conform to the linearity demand and consequently a multivariate model will have to use

more regression factors than is to be expected by the chemical rank (number of components in the mixture).

Scope of this chapter

To study the effect of external variation on the predictive ability of multivariate calibration for spectral data, the temperature has been chosen as the external variable. Short-wave NIR spectra, measured at different temperatures, of mixtures containing ethanol, water and 2-propanol are used as data and PLS regression is employed as data analysis method. Two different types of PLS models are compared: local models that apply to samples of one temperature and global models that can be used for samples at different temperatures. The difference in prediction error for the different models is used to evaluate which calibration strategy can handle temperature-influenced spectra. Explanation of the differences in predictive ability is sought by inspecting the sensitivity vectors for the analytes.

Experimental section

Apparatus

Mixtures of ethanol, water and 2-propanol have been prepared using an analytical balance and kept in airtight sample flasks. Fresh p. a. quality alcohols and sub-boiled water have been used. Closed quartz cells with 1 cm path length have been used in order to prevent dissipation of the alcohols during the measurement. The spectra have been taken on a HP 8453 Spectrophotometer with a thermostatically controlled cell holder and cell stirring module (Hewlett Packard, Palo Alto, CA, USA). The wavelength range used was 580 to 1091 nm with 1 nm resolution and the integration time was 20 s. The collection of the spectra was done on a Hewlett Packard Vectra XM2 PC using the UV-Visible Chemstation software (Rev A.02.04). The temperature of the sample has been regulated using an external Pt-100 sensor immersed in the sample and linked to the controller of a Neslab microprocessor EX-111 circulator bath.

For simulations and the data processing Matlab (ver. 4.2 and 5; The Mathworks Inc.) and the PLS toolbox (ver. 1.4) were used on a Pentium-class computer.

Mixture design

In order to span the concentration variation a mixture design (Figure 2-1) has been set up. The mole fraction levels that obey this design have been mixed and are given in Table 2-1. In order to perform linearity and additivity tests, the spectra of the pure components have also been measured.

The 19 mixtures and the three pure components have been measured at temperatures of 30, 40, 50, 60 and 70 °C (± 0.2 °C).

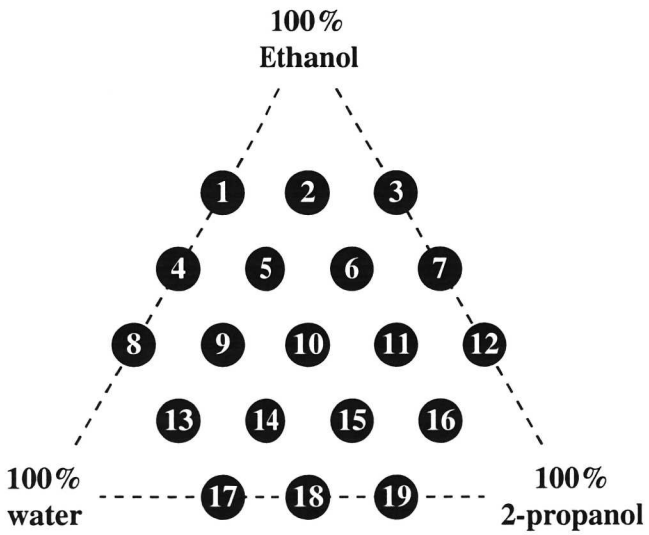

Figure 2-1: Mixture design for ethanol, water and 2-propanol mole fractions.

Table 2-1: Mole-fractions of the samples in %

	ethanol	*water*	*2-prop.*
1	66.4	33.6	0
2	67.2	16.3	16.5
3	66.6	0	33.4
4	50.0	50.0	0
5	50.0	33.3	16.7
6	49.9	16.7	33.3
7	50.0	0	50.0
8	33.3	66.7	0
9	33.2	50.0	16.7
10	33.3	33.4	33.3
11	32.2	16.6	51.2
12	33.5	0	66.5
13	16.6	66.7	16.7
14	16.7	50.0	33.3
15	16.6	33.3	50.1
16	16.2	16.3	67.5
17	0	66.7	33.3
18	0	50.0	50.0
19	0	33.4	66.6

Data analysis

Pretreatment and analysis of experimental data

The measured spectra are pretreated to remove instrumental baseline drift. Straight lines are fitted through the wavelength range 749-849 nm, where no absorbance bands are present, and subtracted from the spectra. The data analysis is performed on the region 850-1049 nm. The absorption at lower wavelengths is too low to be considered significant and absorption above 1050 nm is very noisy due to instrumental effects.

The data analysis consists of PLS1 regressions using the mean-centered pretreated spectra as **X**-block and mean-centered mole fractions for each chemical component separately as **y**-vector. For the different models that will be used the data is always split into a training set for building the respective model and a test set for estimating the predictive quality of that model. When building the model, cross validation techniques are used to estimate the number of latent variables (LV's).

PLS models have been built for each temperature separately (local models) and for the full dataset containing all temperatures (global models). These two cases are fundamentally different when used for prediction of new samples.

Local models

When building small, local models for each temperature it is also necessary to know the temperature of the new samples in the prediction step, otherwise it is not possible to choose one of the local models. If a model and a prediction sample are measured at the same temperature, the mole fraction can directly be predicted (case *a*). Another possibility is that the temperature of the new sample falls in between the model-temperatures (case *b*). In the latter case the estimated concentration of the new sample from one of the models is expected to be biased. In order to achieve a

better prediction, the mole fraction can be estimated by interpolating between the results of the models.

Case *a*: At each temperature models for each chemical compound are built from samples that are on the "edge" of the experimental design (samples 1, 2, 3, 4, 7, 8, 12, 13, 16, 17, 18, 19) and the sample in the "center" (sample 10). The test set is given by the remaining concentration levels (samples 5, 6, 9, 11, 14, 15). As can be seen from the graphical representation in Figure 2-2 A, no extrapolating prediction will be done. The results from local models case *a* can also bee seen as a "best case scenario" considering that temperature does not play any role.

Leave-one-out cross validation is used to establish the number of LV's in all models, using the prediction error for the left-out samples and visual examination of the loading as criteria.

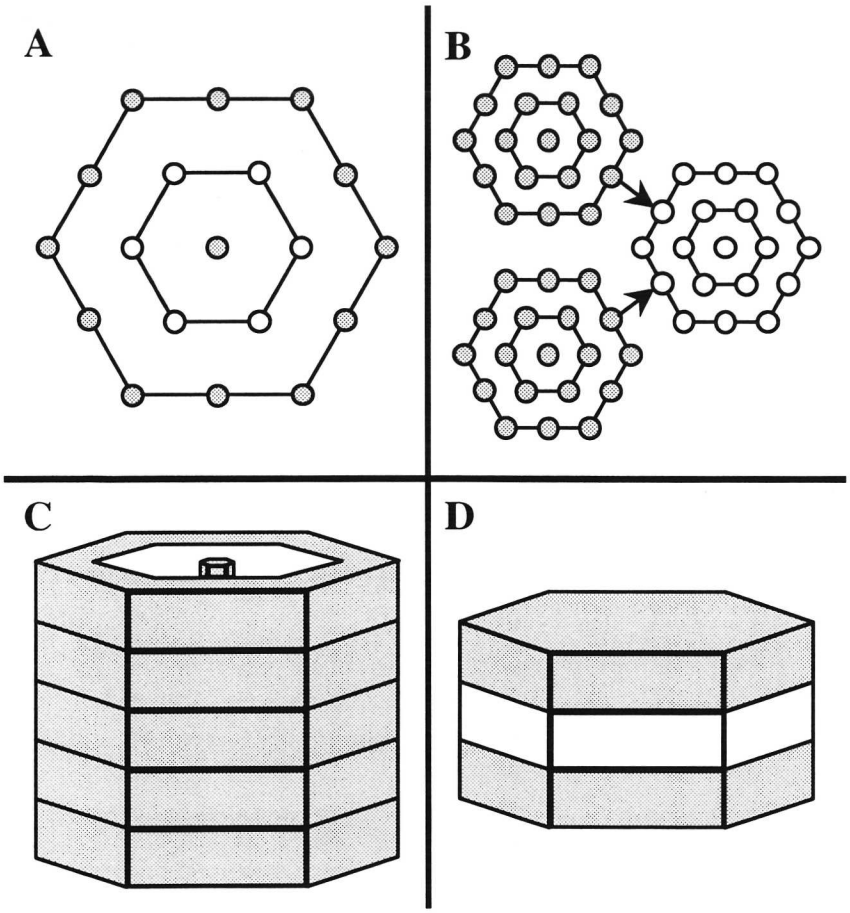

Figure 2-2: Graphical representation of training (gray circles and areas) and test (white circles and areas.) sets. A: Local models case *a*; B: Local models case *b*; C: Global models case *a*; D: Global models case *b*; .

Case *b*: Since the test set consists of samples measured at a different temperature all samples from the experimental design can be used for building the model. Three models are built from the spectra at 30, 50 and 70°C and the prediction samples are the spectra measured at 40 and 60°C (See Figure 2-2 B).

The models are build with the same number of LV's as established for the models in case *a*. The mole fractions of the test set are estimated by averaging the predicted mole fraction resulting from the two models at the nearest temperatures [1].

$$\hat{\mathbf{y}}_{40°C} = \tfrac{1}{2}(\hat{\mathbf{y}}_{30°C} + \hat{\mathbf{y}}_{50°C}) \quad ; \quad \hat{\mathbf{y}}_{60°C} = \tfrac{1}{2}(\hat{\mathbf{y}}_{50°C} + \hat{\mathbf{y}}_{70°C}) \quad [1]$$

Global models

With one global model for all temperatures it is neither necessary to know the temperature of a new sample to be predicted nor that of the training set samples. The global model treats temperature as an unknown interferent. PLS uses the covariance between **X** and **y** to establish a regression model that explains the variation in **y** with variation in **X**. If the spectrum of the interferent correlates perfectly with that of the analyte, the PLS algorithm cannot distinguish between analyte and interferent. The weaker the correlation between interferent and analyte becomes, the easier the PLS algorithm can distinguish between them. The spectrum of temperature (if seen as interferent) is strongly non-linear and different from that of the chemical compounds. It may therefore be advantageous but not necessary to know the temperatures of the training samples and to vary temperature independently from the concentrations in order to minimize the covariance between them.

The differences between a prediction sample with a temperature that "fits" into a model (case *a*) or a sample with a temperature that falls in between models (case *b*) does not apply to general models. The temperature is assumed unknown and the cases can therefore not be distinguished.

For comparison of the predictive abilities however, it is useful to build global models that use exactly the same test and training data as the local models.

Case *a*: The same mixtures are used as training and test sets as in the local models. Instead of building 5 models for the 5 temperatures, all training sample measurements are used to build one global model and to predict all measurements of the test set (see Figure 2-2 C)

Leave more out cross validation was performed on the training set leaving one concentration out for all temperatures at each cross validation step. In this way the disturbance of the design by the left out samples is comparable to that during the cross validation used in the local case. Because of the higher number of training samples it is possible to apply additionally a stratified leave out procedure for verification. The difference between stratified and leave-one-concentration-out strategies is, that with stratified five different mixtures (one per temperature) are left out at random, which is repeated until all concentrations have been left out once for each temperature.

Case *b*: Again the same data is used for training and test sets as with the local models. Two models are made: one using all mixtures at 30 and 50°C for building the model and all mixtures at 40°C for prediction. The other model uses all mixtures at 50 and 70°C as training set and all mixtures at 60°C as test set (see Figure 2-2 D).

The number of LV's used is equal to that of the global model case *a*.

Performance measures

Prediction errors: The root mean squared error (RMSE) is used as performance criterion in cross validation (RMSECV), where it is used to estimate the necessary number of LV's, as well as in prediction (RMSEP), where it is used to asses the predictive power of the model. In both cases the RMSE is calculated in the common way as:

$$RMSE = \sqrt{\frac{\sum_{i=1}^{n}(\hat{y}_i - y_i)^2}{n}} \qquad [2]$$

where $\hat{y}_i$ and y_i are respectively the predicted and real values of sample *i* of the *n* samples in either the cross validation or test set.

In order to place the prediction error in a more recognizable setting the mean relative error (MRE) is also used to summarize the results for each type of model. This way an impression can be given on how many percent the prediction is inaccurate.

Sensitivity vectors: In classical first order univariate calibration the sensitivity is an important characterization of a calibration model. It can be calculated as the difference in net analyte signal (response without the offset) of two measurements at different concentrations resulting in the slope of the calibration line. The higher the sensitivity, the better the model performs, since even slight differences in analyte concentration give a distinctively different response.

Recently a method has been proposed to determine the net analyte signal (NAS) and the sensitivity vector not only for classical univariate and multivariate calibration but also for inverse multivariate calibration methods such as PLS[27]. This extension means that no longer all pure spectra and all concentrations have to be known. The method consists of reconstructing the **X** data (response matrix) by its description used in the calibration model (product of x-loading and x-score blocks). By applying rank annihilation it is possible to eliminate the part of the reconstructed response which is contributed by the analyte. The result is an estimation of the response matrix of only the interferents without the analyte. In classical multivariate calibration the pure spectrum is needed for the rank annihilation step.

Lorber et al.[27] show that a linear combination of mixed spectra can also be used, as long as the analyte is present in those spectra. The NAS can then be estimated as the part of a new measurement that is not described by and therefore orthogonal to the interferents-response matrix. The norm of the NAS vector is (for the linear case) proportional to the concentration. Division of the NAS vector by the sample concentration leads to a sensitivity vector for each of the new measurements. Ideally all sensitivity vectors for new samples are the same but in practice they form only estimates of the concentration-normalized pure spectrum.

When applying net analyte signal, its norm and sensitivity as figures of merit, precautions have to be taken in the case of mean centered data. The linear combination of mixed spectra used in the rank annihilation step cannot be the sum of all spectra from the training set, since they sum up to zero. Therefore spectra with the highest analyte concentration (for ethanol: samples 1, 2, 3; for water: samples 8, 13, 17; for 2-propanol: samples 12, 16, 19) have been chosen. Furthermore, prediction samples with an analyte concentration very near to the mean concentration show a sensitivity vector consisting only of amplified measurement noise, since both NAS and concentration will become almost zero. Because of this artifact, only sensitivity vectors of test samples with a different mole fraction than the mean (one third) and common to all test sets are used for interpretation and comparison (for ethanol: samples 5, 6, 14, 15; for water: samples 6, 9, 11, 14; for 2-propanol: samples 5, 9, 11, 15) .

Results and Discussion

Simulations

To assess the influence of spectral shifts and broadening on multivariate models simulations have been carried out. Especially the increase of complexity (the number of principal components needed to describe the data) was estimated.

Three data sets of Gaussian peaks showing either an increase in area, a shift or changing width were generated and Principal Component Analysis (PCA) was applied to these mean centered datasets. The loadings and scores of the datasets (Figure 2-3) show that only variation in area is a linear phenomenon. Variation in the position of the maximum or in the width of the Gaussian peaks lead to a PCA description with more then one principal component (PC).

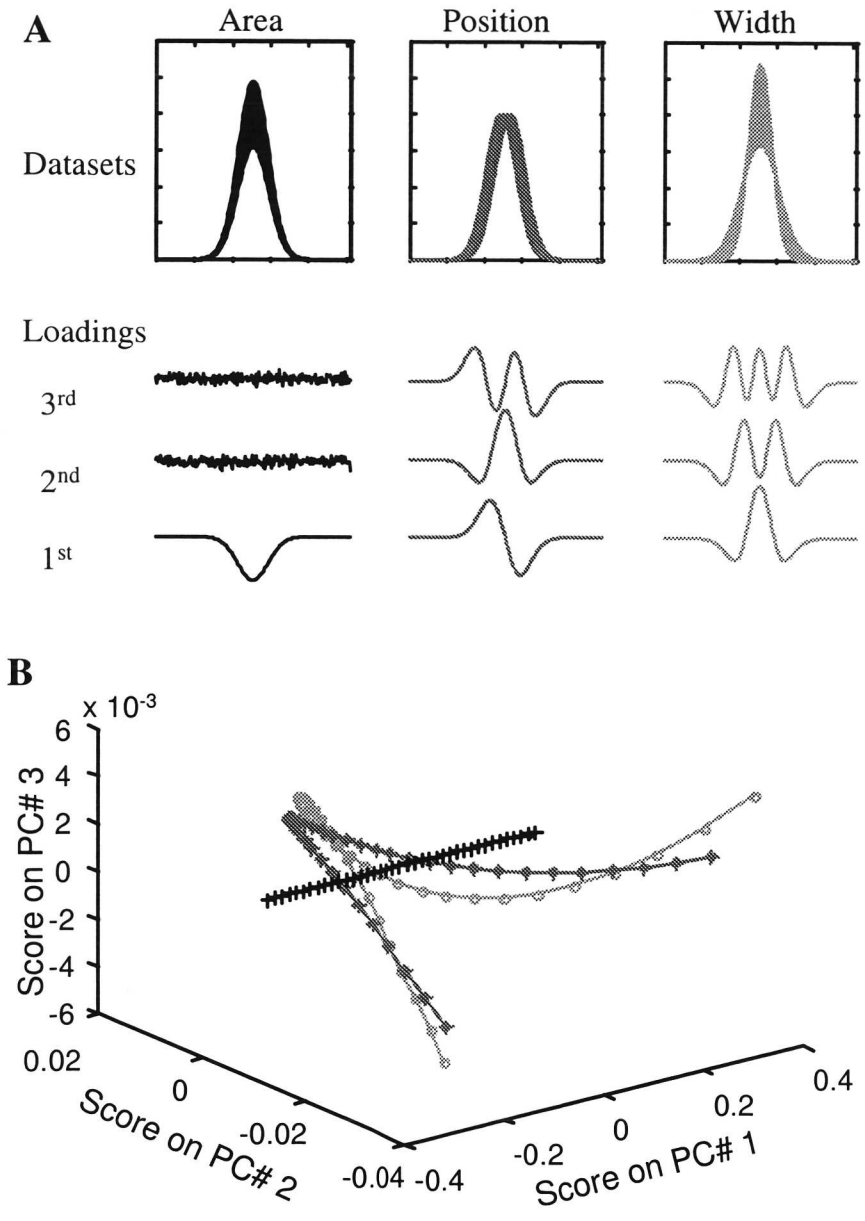

Figure 2-3: Changing area, position and width of a peak and it's effects on multivariate space. *A:* Datasets and loadings. *B:* Score values ++++ Area; ++++Position; ○○○○Width.

It is shown clearly that for the area variation, only the first loading vector has any meaning whilst the second and third merely describe the white noise that has been added. The score plots also show the linearity for the area increase data, since only the first PC contains significant score values.

Contrary, the loadings for the shift and broadening datasets show systematic information even at higher PC's than shown here, until finally noise level is reached. Their respective score plots have a clear 3-D character (corkscrew) since they are non-linear effects and have to be approached by several principal components. An increase in complexity can therefore also be expected for spectra that show shift or broadening of bands.

Qualitative analysis of the data set

Spectra of the pure components have been measured for qualitative evaluation of the temperature effects and testing linearity. Figure 2-4 gives a good impression of the temperature effects on the absorption bands, the band assignments were done using the spectra shown by Bonanno et al.[17]. For water a temperature increase leads to a band shift towards lower wavelengths together with an absorption increase and band narrowing. Rising the temperature decreases the cluster size of hydrogen bonded molecules and increases therefore the fraction of "free" hydroxyls. The alcohols show a very slight decrease of the 3rd C-H overtone, an increase in free O-H and probably some increase in the C-H combination band.

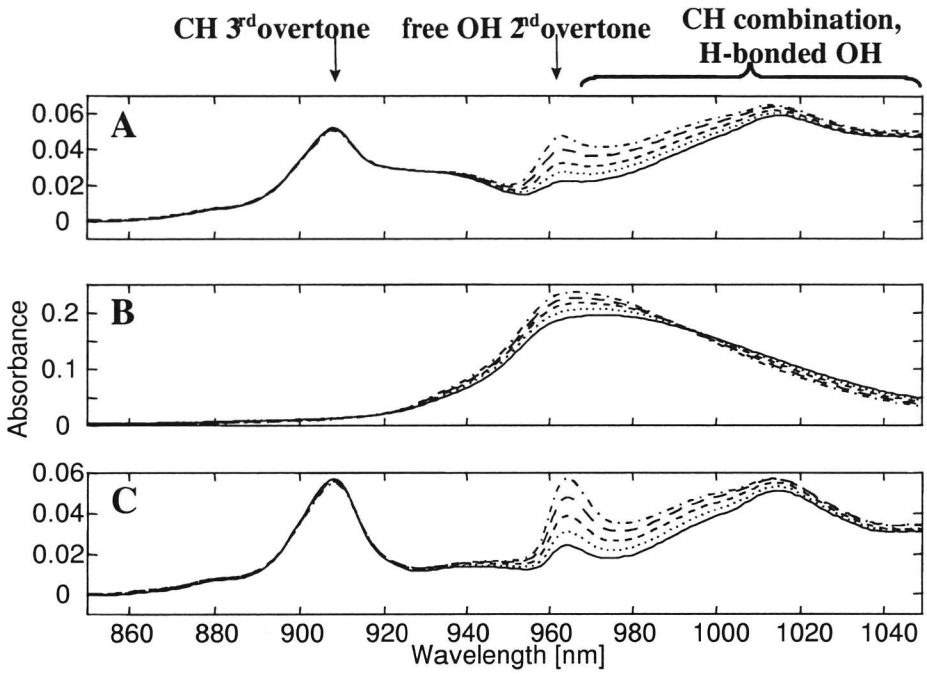

Figure 2-4: Spectra of the pure components at different temperatures (——30 °C ····· 40 °C - - - - 50 °C – – 60 °C and - · - · 70 °C); *A* ethanol, *B* water, *C* 2-propanol

In order to test the linearity and additivity synthetic spectra have been composed by addition of the pure component-spectra multiplied with the concentration levels as in Table 2-1. These synthetic spectra were compared with the measured spectra. In Figure 2-5 the differences between some synthetic and real spectra are shown. Deviation from linearity and additivity were especially found with mixtures containing a high fraction of water (sample 13). In comparison, the differences between the real and the synthetic spectra were much smaller for mixtures without water (sample 7).

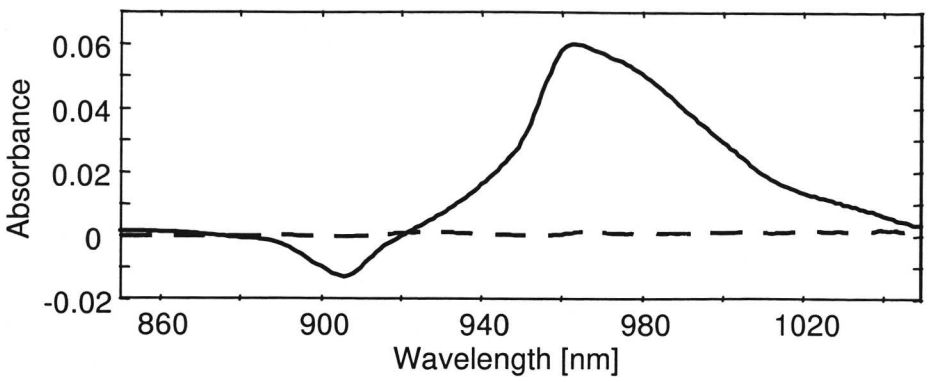

Figure 2-5: Difference between real and synthetic spectra. Solid line sample: 13 ($^1/_6$ ethanol, $^2/_3$ water, $^1/_6$ 2-propanol). Dashed line: sample 7 (½ ethanol / ½ 2-propanol) .

A PLS regression of the spectra on their mole fractions is therefore expected to need more LV's than would be expected by the chemical rank[28].

Local models

Case *a*: Leave one out cross-validation is performed on the training set (see Figure 2-2) for calibration models for each of the three chemical compounds at each of the 5 temperatures.

For all local models the RMSECV does decrease considerably until 4 LV's are included, staying more or less constant for more LV's. The models for water give an about factor three lower RMSECV but show the same behavior. This is due to the fact that water has a higher absorption in the wavelength range studied than the alcohols.

Visual inspection of the loading plots indicates for all models that only the first four loadings show systematic spectral information; higher LV's consist primarily of noise. Therefore, 4 LV's have been used to build the PLS-models for predicting the mole fractions in the test set. Note that in the ideal

case (linearity and additivity) the model would only consist of two LV's since the chemical rank is two (3 components with closure) and the spectra are mean centered [29]. The non-additive behavior of especially water is responsible for the higher number of LV's necessary in practice.

The individual predicted mole fractions for each test sample and temperature did not show any anomalies such as outliers or systematic errors. The results will therefore be summarized by giving the values for the RMSEP and MRE per model only (see Table 2-2). The error for the prediction of water is considerably lower than for the alcohols. On the average a prediction for one of the components at any temperature would be about 3% inaccurate.

Table 2-2: RMSEP ($\cdot 10^{-2}$) and MRE for the different models.

	Temperature [°C] of		ethanol		water		2-propanol	
	Sample	Model	RMSEP	MRE	RMSEP	MRE	RMSEP	MRE
Local a	30	30	1.77	4.0%	0.92	3.2%	1.24	3.2%
	40	40	1.06	2.1%	0.67	1.3%	0.93	2.4%
	50	50	1.66	4.0%	1.11	2.8%	2.18	7.4%
	60	60	0.98	3.0%	0.43	1.4%	0.83	2.3%
	70	70	1.12	3.4%	0.38	1.3%	1.47	2.5%
		Mean	**1.32**	**3.3%**	**0.70**	**2.0%**	**1.33**	**3.6%**
Local b	40	30 & 50	1.81	3.8%	0.51	1.4%	2.74	7.5%
	60	50 & 70	2.77	8.5%	1.13	3.1%	1.92	5.6%
		Mean	**2.29**	**6.1%**	**0.82**	**2.3%**	**2.33**	**6.5%**
Global a	30	30-70	1.38	4.9%	1.25	3.4%	1.13	3.1%
	40	30-70	1.32	5.0%	0.55	1.9%	1.64	5.1%
	50	30-70	3.77	13.1%	0.79	2.3%	4.08	14.9%
	60	30-70	1.59	5.5%	0.84	3.1%	1.74	4.0%
	70	30-70	1.75	4.9%	0.76	2.1%	1.75	4.6%
		Mean	**1.96**	**6.7%**	**0.84**	**2.6%**	**2.07**	**6.3%**
Global b	40	30 & 50	1.17	3.4%	0.95	2.9%	1.03	2.2%
	60	50 & 70	1.24	4.4%	0.93	2.1%	1.30	3.7%
		Mean	**1.21**	**3.9%**	**0.94**	**2.5%**	**1.17**	**3.0%**

The higher signal of water translates to a higher norm of the NAS's and sensitivities for water (Table 2-3). The increase in absorption with the increase in temperature for all three components (Figure 2-4) also gives rise to higher sensitivity at higher temperatures. The sensitivity vectors for all samples (except the samples with mole fraction 1/3 as explained in Performance measures) are very similar, as shown for ethanol in Figure 2-6a.

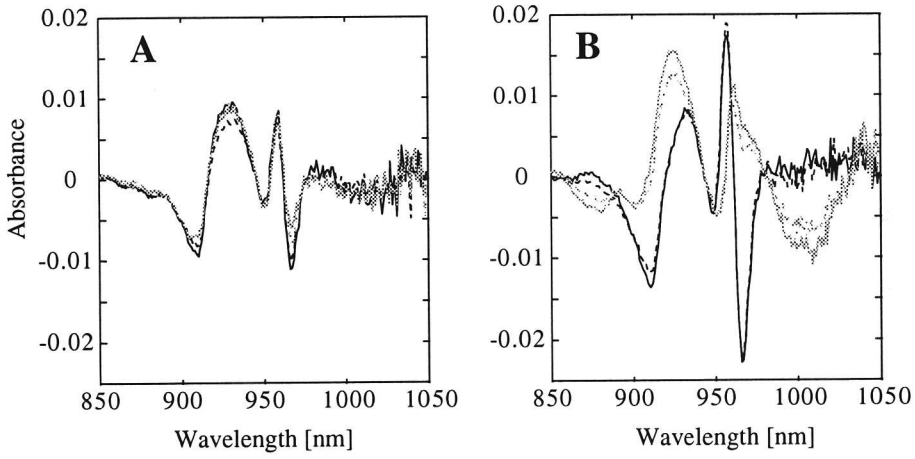

Figure 2-6: Sensitivity vector plots for ethanol prediction of samples —5, - -6, ⋯14 and ⋯15 measured at 40℃. *A*: Local model case *a* at 40℃. *B*: Local model case *b*, vectors (model at 30℃).

Table 2-3: Norm of the sensitivities for prediction samples: 5, 6, 14 ,15 for ethanol, 6, 9, 11, 14 for water and 5, 9, 11, 15 for 2-propanol.

		Temperature [°C] of		Sensitivity norm ($\cdot 10^{-2}$) for:		
		Sample	Model	ethanol	water	2-prop
Local	a	30°C	30°C	5.60	9.33	6.47
		40°C	40°C	5.40	10.6	6.47
		50°C	50°C	5.77	10.4	6.54
		60°C	60°C	5.81	12.3	7.20
		70°C	70°C	6.56	13.4	8.47
			Mean	**5.83**	**11.2**	**7.03**
	b	40°C	30°C	8.45	12.3	9.61
		40°C	50°C	8.35	11.2	7.62
		60°C	50°C	7.68	13.0	9.55
		60°C	70°C	10.0	14.0	9.64
			Mean	**8.63**	**12.7**	**9.11**
Global	a	30°C	30-70°C	3.46	7.32	3.10
		40°C	30-70°C	4.00	7.33	3.37
		50°C	30-70°C	3.77	7.20	3.09
		60°C	30-70°C	3.66	7.54	3.09
		70°C	30-70°C	3.67	7.72	3.35
			Mean	**3.71**	**7.42**	**3.20**
	b	40°C	30 & 50°C	3.97	8.47	3.64
		60°C	50 & 70°C	3.83	7.89	3.25
			Mean	**3.90**	**8.18**	**3.45**

Case *b*: With these models predictions for a test temperature are calculated as the average prediction based on local models built for the two "neighboring" temperatures. The prediction errors found are given in Table 2-2.

The models can obviously not predict with a good accuracy measurements done at a different temperature. Averaging the predicted mole fraction improves the prediction error to approximately half of the prediction error given by the PLS models at the two nearest temperatures. Still, the prediction errors are almost twice as high as in case *a*.

The sensitivities (Table 2-3) are higher than for local models case *a*. This is due to the fact that the NAS does not describe only the analyte but also the temperature difference between the training set and prediction samples. This is shown by comparing the plots in Figure 2-6, revealing the difference between the sensitivities of case *a* and *b*. The same test samples measured at 40°C exhibit very different and irregular sensitivity vectors when predicted by a model at 30°C. The rank annihilation step causes the net analyte signal to describe everything except absorption due to water and 2-propanol at 30°C. The difference between the sensitivities for samples 5,6 and 14,15 shows clearly that the temperature effect, now incorrectly included in the NAS and sensitivities, is dependent on the concentrations.

Global models

Case *a*: The training set for all five temperatures is used to build the model and the mole fractions of the test set at all temperatures are predicted.

For both cross validation strategies the RMSECV steadily decreases with the number of LV's up to seven LV's included in the model when it stops decreasing significantly. The loading plots show that the LV's higher than seven describe mostly noise. Therefore models with 7 latent variables were built form the training sets.

Apparently, the nonlinearity of the temperature effects forces the PLS algorithm to model some systematic information in such high LV's. Roughly, the number of LV's can be rationalized as two LV's necessary to describe the chemical problem, two further to explain the non-additive behavior of water (see local models) and three more LV's for the description of the nonlinearities due to temperature variation.

The prediction errors for the test set at the different temperatures are given in Table 2-2. In absolute terms (RMSEP) the global model performs worse than the local model case a and comparable to case *b*. The high mean relative error compared to the equivalent predictions by the local models is caused by the fact that the model makes a relative high error when predicting lower mole fractions.

The norms of the sensitivity vectors (Table 2-3) are considerably lower than those for the local models. This leads to the conclusion that, due to the variation caused by temperature, the model is forced to use a smaller amount of the spectra for prediction of the analyte.

Case *b*: In this case data at two temperatures (30 and 50 °C or 50 and 70 °C) are used for building a model and the spectra at the temperature in between (40 or 60 °C resp.) are used as prediction set. As it was the case for the local models, the global models case *b* are built with the same number of LV's (7) as in case *a*. Table 2-2 displays the RMSEP and MRE values for the two test sets. When compared to the results of the corresponding local model, the global model predicts more accurate in almost all cases. As a whole, the predictive performance is comparable to that of local models case *a*, being slightly better for the alcohols and slightly worse for water. Considering that the local models are in a way a "best case scenario" it means that the temperature effect on the predictions is reduced to a minimum.

The sensitivity-norms (Table 2-3) are only little higher than for global models case *a*, especially for the test set at 40°C predicted with the spectra at 30 and 50°C. The smaller temperature span and mainly the higher number of calibration samples improves the predictive ability in comparison to case *a*. Still, a considerable part of a spectrum is not used for prediction due to the temperature effects as can be seen from comparing the sensitivity-norms with the local model case *a*.

Conclusions

Global models in which the temperature is modeled as an unknown interferent perform only slightly inferior to local models which are calibrated and used for a specific temperature. Global models, however, have a tendency to become (very) complex. The obtained global models needed seven LV's, three to describe the temperature interference, two for the non-additive behavior of water whilst the chemical system is of rank two. If temperature is treated as an unknown interferent, it is more important to span the variation due to concentration rather than for many temperature levels.

Interpolation between local models, to accommodate temperatures not present in the calibration set, performs poorly.

Further research will aim to describe the temperature effects explicitly; either by preprocessing data before calibration or by inclusion of temperature into a calibration model itself.

References

[1] Blaser, W. W.; Bredeweg, R. A.; Harner, R.S.; LaPack, M.A.; Leugers, A.; Martin, D. P.; Pell, R. J.; Workman, J., Jr.; Wright, L. G. *Anal. Chem.* **1995**, *67*, 47R-70R.

[2] DeThomas, F. A.; Hall, J. W.; Monfre, S.L. *Talanta* **1994**, *41*, 425-431.

[3] Frank, I. E.; Feikema, J.; Constantine, N.; Kowalski, B. R. *J. Chem. Inf. Comput. Sci.* **1984**, *24*, 20-24.

[4] Hall, J. W.; McNeil, B.; Rollins, M. J.; Draper, I.; Thompson, B. G.; Macaloney, G.; *Appl. Spectrosc.* **1996**, *50*, 102-108.

[5] Siesler, H.W. *Landbauforschung Völkenrode*, **1989**, 112-118.

[6] Hildrum, K.I.; Isaksson, T.; Næs, T.; Tandberg, A. *Near Infrared Spectroscopy: Bridging the Gap between Data Analysis and NIR Applications*; Ellis Horwood: New York, 1992.

[7] Burns, D. A.; Ciurczak, E.W. *Handbook of Near-Infrared Analysis*, 1st edition; Marcel Dekker Inc.: New York, 1992.

[8] Cho, T.; Kida, I.; Ninomiya, J.; Ikawa, S. *J. Chem. Soc. Faraday Trans.* **1994**, *90*, 103-107.

[9] Czarnecki, M.A.; Czarnecka, M.; Ozaki, Y. *Spectrochim. Acta*, **1994**, *50*, 1521-1528.

[10] Czarnecki, M.A.; Liu, Y.; Ozaki, Y.; Suzuki, M.; Iwahashi, M. *Appl. Spectrosc.* **1993**, *47*, 2162-2168.

[11] Hazen, K. H.; Arnold, M. A.; Small, G. W. *Appl. Spectrosc.* **1994**, *48*, 477-483.

[12] Kamiya, N.; Sekigawa, T.; Ikawa, S. *J. Chem. Soc. Faraday Trans.* **1993**, *89*, 489-493.

[13] Liu, Y.; Czarnecki, M.A.; Ozaki, Y.; Suzuki, M.; Iwahashi, M. *Appl. Spectrosc.* **1993**, *47*, 2169-2171.

[14] de Noord, O.N. *Chemom. Intell. Lab. Syst.* **1994**, *25*, 85-97.

[15] Okuyama, M.; Ikawa, S. *J. Chem. Soc. Faraday Trans.* **1994**, *90*, 3065-3069.

[16] Ozaki, Y.; Liu, Y.; Noda, I. *Appl. Spectrosc.* **1997**, *51*, 526-535.

[17] Bonanno, A.S.; Olinger, J.M.; Griffiths, P.R. *in [6].*

[18] Libnau, F.O.; Kvalheim, O.M.; Christy, A. A.; Toft, J. *Vib. Spectrosc.* **1994**, *7*, 243-254.

[19] Pegau, W. S.; Zaneveld, J. R. V. *Limnol. Oceanogr.* **1993**, *38*, 188-192.

[20] Finch, J. N.; Lippincott,k E. R. *J. Chem. Phys.*, **1956**, *24*, 908-909.

[21] Finch, J. N.; Lippincott,k E. R. *Phys. Chem.* , **1957**, *61*, 894-902.

[22] Kemeny, G. J. *in [7].*

[23] Noda, I. ; Liu, Y.; Ozaki, Y.; Czarnecki, M.A. *J. Phys. Chem.* **1995**, *99*, 3068-3073.

[24] Liu, Y. ; Czarnecki, M.A.; Ozaki, Y. *Appl. Spectrosc.* **1994**, *48*, 1095-1101.

[25] Wang, F.C.; Feve, M.; Lam, T. M.; Pascault, J. P. *J. Polym. Sci.: Phys.* **1994**, *32*, 1305-1313.

[26] Eschenauer, U.; Henck, O.; Hühne, M.; Wu, P.; Zegber, I.; Siesler, H. W. *in [6].*

[27] Lorber A.; Faber, K.; Kowalski, B.R. *Anal. Chem.* **1997**. *69*, 1620-1626.

[28] DiFoggio, R. *Appl. Spectrosc.* **1995**, *49*, 67-75.

[29] Pell, R. J.; Seasholtz, M. B.; Kowalski, B. R. *J. Cemom.* **1992**, *6*, 57-62.